Computational alignment of on-machine deflectometry

Kang, Hyukmo, Quach, Henry, Choi, Heejoo, Smith, Greg, Kim, Dae Wook

Hyukmo Kang, Henry Quach, Heejoo Choi, Greg A. Smith, Dae Wook Kim, "Computational alignment of on-machine deflectometry," Proc. SPIE 11487, Optical Manufacturing and Testing XIII, 114870O (20 August 2020); doi: 10.1117/12.2576955

SPIE.

Event: SPIE Optical Engineering + Applications, 2020, Online Only

Computational alignment of on-machine deflectometry

Hyukmo Kang[a], Henry Quach[a], Heejoo Choi[a,b], Greg A. Smith[a], and Dae Wook Kim[a,b,c,*]

[a]Wyant College of Optical Sciences, University of Arizona, 1630 E. University Blvd., Tucson, AZ 85721 USA

[b]Large Binocular Telescope Observatory, 933 N. Cherry Ave., Tucson, AZ, 85721 USA

[c]Department of Astronomy and Steward Observatory, University of Arizona, 933 N. Cherry Ave., Tucson, AZ 85721, USA

ABSTRACT

Accurate system calibration remains an area of active improvement in deflectometry. Since deflectometry requires the geometry information of all participating hardware to be well known, miscalibration can mar the accuracy of surface reconstruction especially in lower order shapes. To uphold reconstruction fidelity, extra measuring instruments (i.e. coordinate measuring machines, laser trackers, metering rods) or reference features (i.e. fiducial points or reference mirror) to find out the positions of a camera, a screen, and a unit under test are used. These methods provide reliable calibration but are resource-intensive. In this paper, we introduce an alignment algorithm to calibrate the geometry of a deflectometry configuration. We leverage the concept of alignment algorithm which uses a sensitivity model. With the aid of ray tracing simulation, the relationship between camera pixels and screen pixels of a deflectometer is quantitatively established. This pixel-to-pixel relationship enables us to generate computational imaging of screen and characterize the tendency of misalignments of the deflectometer. On top of that, we can calculate and make multiplexed patterns of screen which highlight the effect of misalignments. We set specific indices and corresponding screen patterns for each alignment parameters to build the sensitivity model. The initial simulation result shows that the algorithm can estimate misalignment status. We believe that this algorithm can be an alternative and efficient calibration process for the deflectometry system, especially when the usage of extra measuring devices is limited.

Keywords: Deflectometry, Alignment, On-machine metrology, Calibration, Computational imaging

1. INTRODUCTION

Deflectometry is an attractive solution for on-machine metrology as it has a high slope measurement range, does not require a physical null reference.[1,2] However, obtaining reliable geometrical information for a deflectometry system is critical for high surface reconstruction accuracy, and imprecise calibration can significantly alter lower order shapes. To uphold reconstruction fidelity, extra measuring devices (i.e. coordinate measuring machines, laser trackers, metering rods) or reference features (i.e. fiducial points or reference mirror) are used to find the geometry of the deflectometry system.[3,4] For an on-machine deflectometer mounted on a computer numerically controlled (CNC) machine, we can easily and precisely obtain the position of the unit under test (UUT), but the relative position between UUT and deflectometer hardware remains uncertain. Furthermore, due to machine costs or the size of the UUT, an external measuring device is not always available.

*E-mail: letter2dwk@hotmail.com

Optical Manufacturing and Testing XIII, edited by Dae Wook Kim, Rolf Rascher,
Proc. of SPIE Vol. 11487, 114870O · © 2020 SPIE · CCC code:
0277-786X/20/$21 · doi: 10.1117/12.2576955

2. DEFLECTOMETRY SIMULATOR AND ALIGNMENT ALGORITHM

2.1 Deflectometry Simulator

Deflectometry uses the local slope of the optic obtained from a point-to-point correspondence between the planes of the screen, UUT, and detector (Fig. 1). With the aid of ray tracing programs, we establish relationship between the screen, UUT, and detector pixels. After obtaining relationships in multiple scenario (e.g. misalignment), we applied a linear fitting to determine the pair coordinates of screen and detector pixels. This virtual deflectometry simulator (Fig. 2) enables us to characterize misalignments within the deflectometer and surface figure error of the UUT. This simulator has the potential to be applicable towards many deflectometry experiments beyond just alignment, including surface reconstruction and result validation.

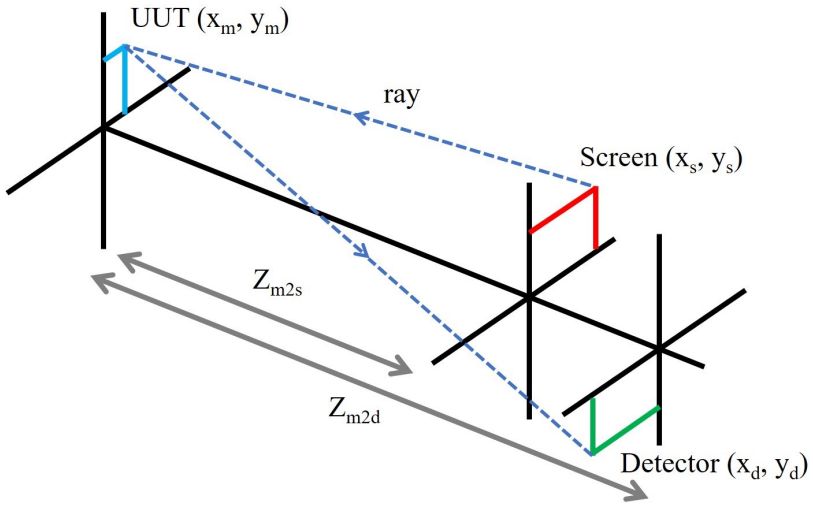

Figure 1. Simple diagram of a deflectometry system.[5] The path of a single ray traced in the deflectometry system. To obtain local slope of UUT, we need the coordinates of screen pixel (x_s, y_s), detector pixel (x_d, y_d), sampled position (x_m, y_m), and distances along the optical axis from UUT to screen and detector, Z_{m2s}, Z_{m2d}.

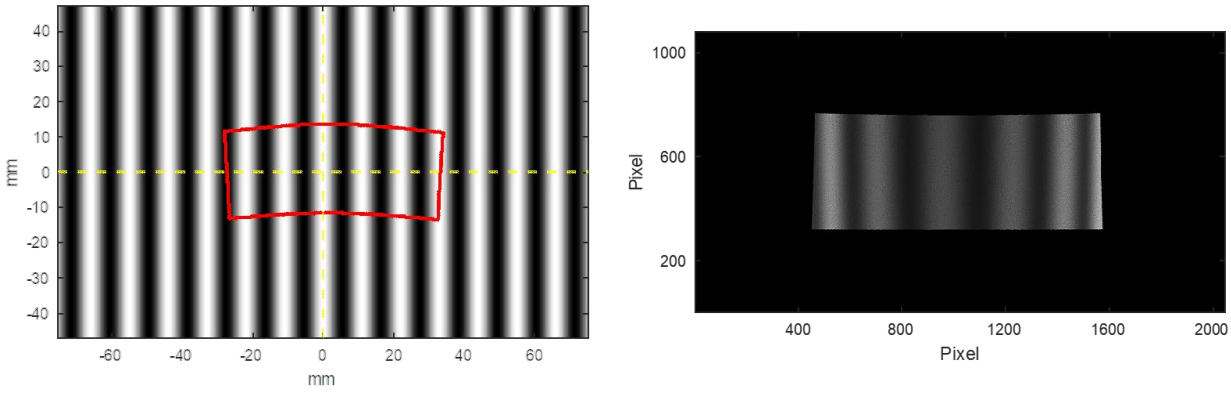

(a) (b)

Figure 2. Example images from the deflectometry simulator. (a) Sinusoidal pattern is displayed on the screen, and the red outline shows corresponding region to shine the UUT. (b) Image of UUT at the conjugated camera detector plane.

2.2 Sensitivity Matrix

The reverse-optimization algorithm is a widely used method to align optical system.[6–8] This method estimates the misalignments by measuring the wavefront errors or Zernike coefficients at multiple fields (ΔZ), then applying the measured parameters to the theoretical sensitivity matrix (S) to quantify the amount of misalignment (ΔD). For n Zernike terms and m misalignment parameters, it can be expressed as

$$\Delta Z = S\Delta D, \qquad where$$

$$\Delta Z = \begin{bmatrix} \Delta Z_1 \\ \vdots \\ \Delta Z_n \end{bmatrix} = \begin{bmatrix} Z_1 \\ \vdots \\ Z_n \end{bmatrix} - \begin{bmatrix} Z_{1o} \\ \vdots \\ Z_{no} \end{bmatrix}, S = \begin{bmatrix} \frac{\delta Z_1}{\delta x_1} \cdots \frac{\delta Z_1}{\delta x_m} \\ \vdots \\ \frac{\delta Z_n}{\delta x_1} \cdots \frac{\delta Z_n}{\delta x_m} \end{bmatrix}, \Delta D = \begin{bmatrix} \Delta x_1 \\ \vdots \\ \Delta x_n \end{bmatrix} = \begin{bmatrix} x_1 \\ \vdots \\ x_n \end{bmatrix} - \begin{bmatrix} x_{1o} \\ \vdots \\ x_{no} \end{bmatrix}. \quad (1)$$

In practice this approach shows convergence of misalignment values after iterative alignment if the sensitivity is linear. To utilize this approach, finding linear sensitive indicators for the computational deflectometry alignment process is essential, which are discussed in chapter 3.2.

3. COMPUTATIONAL ALIGNMENT SIMULATION

3.1 End-to-end simulation setup

We developed and built the deflectometry model simulation analyze algorithm. In this simulation, we set the deflectometer to have a screen size 7 inches across the diagonal with resolution of 1920×1080 pixels and a 2MP color camera located 10 mm above the screen where both centers lie on the Y axis. We utilized a freeform mirror with rectangular aperture (Tab. 1). The center of the UUT lies on the Z axis 200 mm away from the camera and is slightly tilted such that the screen fills the field of view. The overall simulation layout is shown in Fig. 3.

Table 1. Specification of the UUT

Surface Type	X Width	Y Width	X Radius of Curvature	Y Radius of Curvature	X Conic Constant	Y Conic Constant
Bi-aspheric	60 mm	24 mm	150 mm	400 mm	4	-2

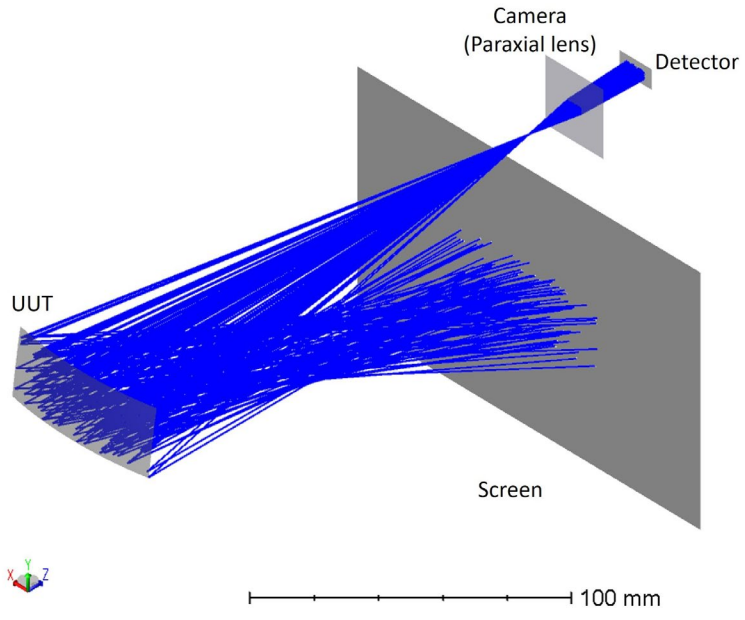

Figure 3. Layout of the deflectometry simulation. Camera and the center of UUT are aligned along the Z-axis for symmetry.

3.2 Alignment parameters

The alignment parameters utilized in the sensitivity matrix require two features to be effective; i) Linearity for misalignment ii) Orthogonality between different degree of freedoms. We must consider these features to correctly set the indices and corresponding screen patterns for each alignment parameter to highlight the effects of misalignments. For X and Y translation of the UUT against deflectometry system (Dx, Dy) we set X and Y centroid position of UUT image as alignment parameters. For Z translation (Dz), we set the image size at the camera sensor as alignment parameter. Generally, it is hard to distinguish between translation and tilt while watching the UUT image via camera because they show similar aspects in deviation. However, contrary to the translation, tilting uses a smaller region on screen to shine the UUT due to the projection (Fig. 4). We find that the rgb-triplet values could be used as an alignment parameter to separate tilt from translation. In this simulation, the binary red/blue pattern on the screen and recorded r/b ratio (in terms of areas on detector) shows sensitivity to tilt in X and Y (Tx, Ty). (Fig. 5 (a),(b)) For the tilt in Z (Tz, clocking of the UUT), we displayed a rgb pattern (similar to Bayer filter layout) and used g-value (i.e., green area on detector) itself as the alignment parameter (Fig. 5(c)). We investigated how each of the alignment parameters are changing from -1 mm to 1 mm in translation, and from -1 degree to 1 degree in tilt using Zemax OpticStudio, and linear fitting. The linear fitting coefficients are shown in Tab. 2.

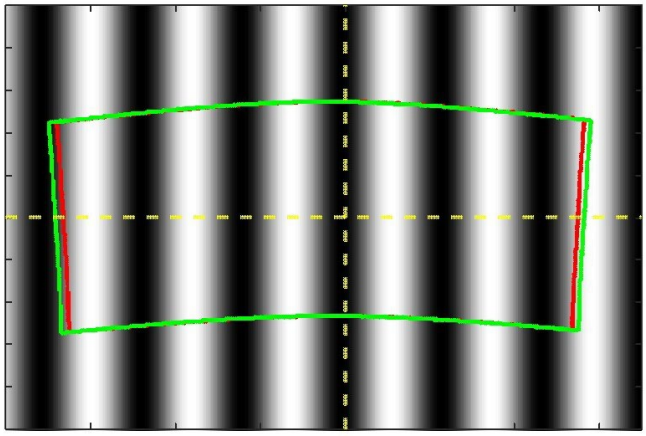

Figure 4. Effective area of screen when perturb the UUT with translation in X (red outline) and tilt in Y (green outline). The position of effective area is similar, but different in size especially in horizontal direction.

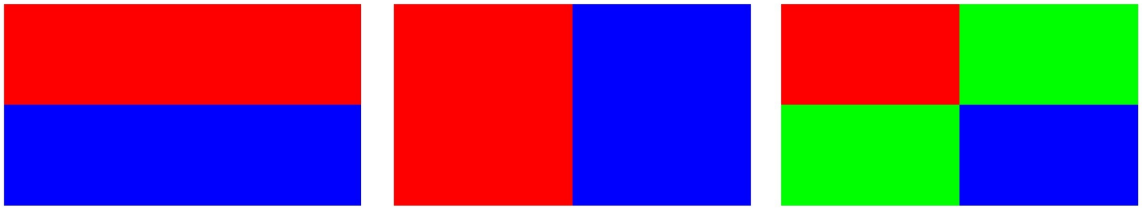

(a) (b) (c)

Figure 5. Color patterns that used to define alignment parameters for tilt. (a) Tilt in X (Tx) (b) Tilt in Y (Ty) (c) Tilt in Z (Tz)

Sensitivity graphs of X centroid and r/b ratio for left-right color pattern are shown in Fig. 6 and Fig. 7 as examples. In Fig. 6, translation in X is most sensitive, and other degree of freedoms are negligible. In Fig. 7, tilt in Y shows most rapid slope, but translation in X also has some gradient. This coupling effect would affect the performance of alignment state estimation. However, since the slope is 5 times greater, and the translation in X would be corrected by other parameter (X centroid), we could mitigate the coupling effect by iteration. The effect of imperfect linearity in tilt in Y also can be relieved by iteration.

Table 2. Sensitivity table for all possible degree of freedom. Highlighted cells mean the most sensitive degree of freedom for each alignment parameters that will be used as indicator.

DoF	Cen.X	Cen.Y	Img. Size	r/b (a)	r/b (b)	g
Dx	-22.50	0.00	-0.02	0.00	0.10	0.01
Dy	-0.03	-22.93	0.50	-0.32	0.00	0.00
Dz	0.01	-0.06	5.01	-0.03	0.00	0.00
Tx	0.00	0.60	-1.74	1.86	0.00	0.00
Ty	0.69	-0.01	0.06	0.00	0.53	0.00
Tz	-0.09	-0.03	-0.07	0.00	0.03	-0.02

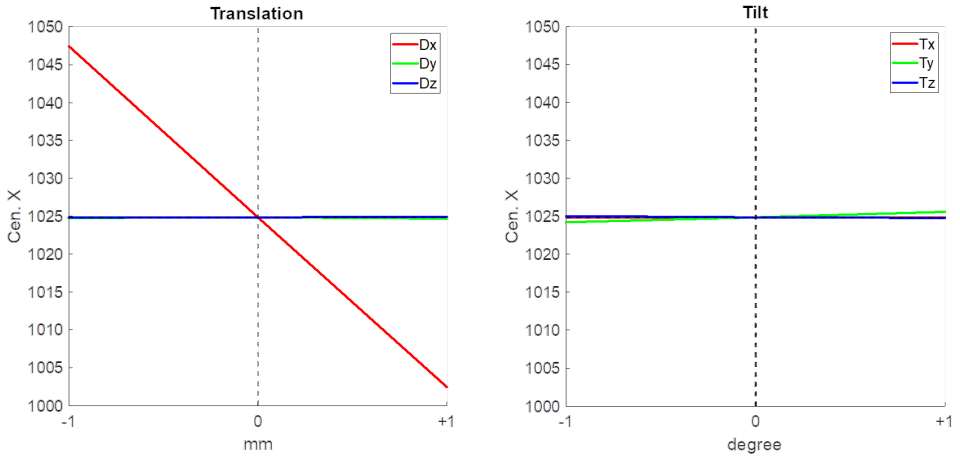

Figure 6. Sensitivity trend plots of X-centroid for all misalignment cases. Translation in X shows most sensitivity, and other misalignments have negligible slopes.

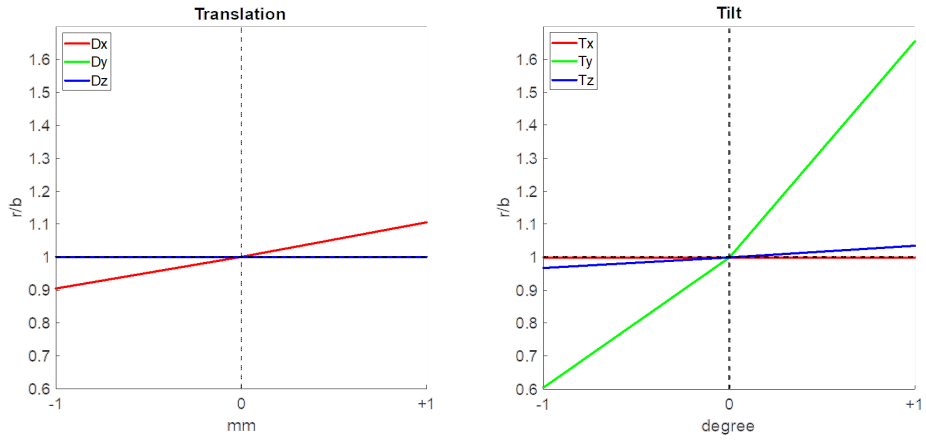

Figure 7. Sensitivity trend plots of r/b ratio when Fig. 5(b) is used. Tilt in Y shows most sensitivity compared to other misalignments. The effects of coupling and insufficient linearity could be mitigated by iterative alignment steps.

3.3 Iterative alignment process simulation

Fig. 8 shows the results of an iterative alignment process simulation assuming an on-machine alignment using the CNC machine axis in each iteration. We imposed random initial misalignment errors to the UUT position and utilized our simulator to obtain the misalignment amount for all degree of freedoms, simultaneously. As a result, calculated misalignment values are converged in induced initial errors after 7 iterations. Dx and Dy converged faster due to their higher sensitivities. Ty and Tz converged shortly after Dx, since Dx disturbs both the r/b ratio and g value. Finally, Dz and Tx converge, but are not fully corrected; however, the converged values for Dz and Tx are within the regime of mechanical error.

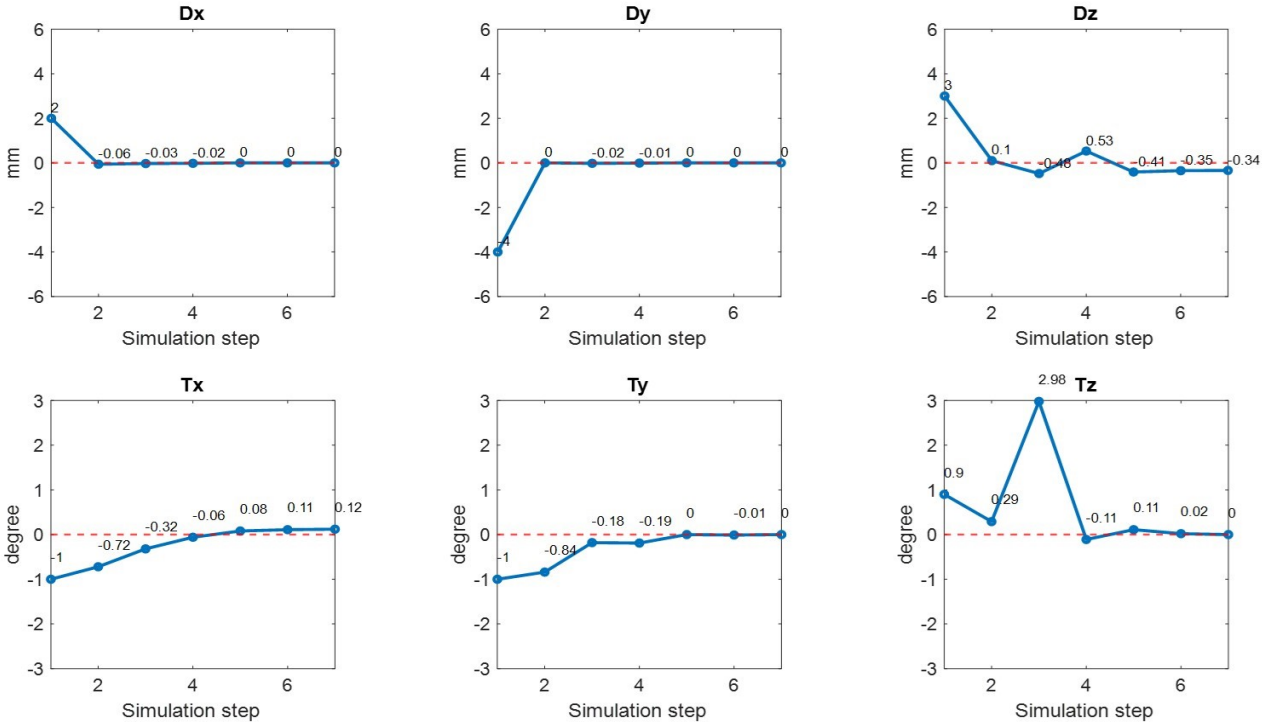

Figure 8. Iterative on-machine deflectometry alignment simulation results using the proposed computational alignment method. After 7 times of iteration, all alignment parameters are successfully converged. As the parameter for Tz is also varies with Dx and the sensitivity is similar (Tab. 2), it shows spike in third iteration step. However, after Dx is corrected, Tz is corrected and converged as well.

4. CONCLUSION

A computational alignment algorithm to calibrate the geometry of a deflectometry configuration is introduced and simulated. We obtained the required pixel-to-pixel relationship between the detector, UUT, and screen using ray tracing programs. Then set specific indices and corresponding screen patterns to determine the effect of misalignments for each degree of freedom. The initial simulation result shows that the algorithm can estimate each misalignment for each degree of freedom and provide a convergent solution for *all* degree of freedoms. This algorithm can be used as an efficient alternative calibration process for deflectometry systems, especially when the usage of extra measuring devices is limited and the CNC machine axis can provide precise alignment adjustments. We plan to perform further error analysis including other calibration errors, and apply the algorithm to an actual measurement process.

ACKNOWLEDGMENTS

The authors would like to acknowledge the II-VI Foundation Block-Gift Program for helping support general deflectometry research in the LOFT group. A special thank you goes to John Kam who helped edit and gave feedback on the article.

REFERENCES

[1] Su, P., Parks, R. E., Wang, L., Angel, R. P., and Burge, J. H., "Software configurable optical test system: a computerized reverse hartmann test," *Appl. Opt.* **49**, 4404–4412 (Aug 2010).

[2] Su, P., Wang, S., Khreishi, M., Wang, Y., Su, T., Zhou, P., Parks, R. E., Law, K., Rascon, M., Zobrist, T., Martin, H., and Burge, J. H., "SCOTS: a reverse Hartmann test with high dynamic range for Giant Magellan Telescope primary mirror segments," in [*Modern Technologies in Space- and Ground-based Telescopes and Instrumentation II*], Navarro, R., Cunningham, C. R., and Prieto, E., eds., **8450**, 332 – 340, International Society for Optics and Photonics, SPIE (2012).

[3] Huang, R., Su, P., Burge, J. H., Huang, L., and Idir, M., "High-accuracy aspheric x-ray mirror metrology using software configurable optical test system/deflectometry," *Optical Engineering* **54**(8), 084103 (2015).

[4] Su, P., Khreishi, M., Huang, R., Su, T., and Burge, J. H., "Precision aspheric optics testing with SCOTS: a deflectometry approach," in [*Optical Measurement Systems for Industrial Inspection VIII*], Lehmann, P. H., Osten, W., and Albertazzi, A., eds., **8788**, 392 – 398, International Society for Optics and Photonics, SPIE (2013).

[5] Kam, J., "Differential phase measuring deflectometry for high-sag freeform optics," (2019).

[6] Figoski, J. W., Shrode, T. E., and Moore, G. F., "Computer-aided alignment of a wide-field, three-mirror, unobscured, high-resolution sensor," in [*Recent trends in Optical systems design and computer lens design workshop II*], **1049**, 166–177, International Society for Optics and Photonics (1989).

[7] Zhang, B., Zhang, X., Wang, C., and Han, C., "Computer-aided alignment of the complex optical system," in [*Advanced Optical Manufacturing and Testing Technology 2000*], **4231**, 67–72, International Society for Optics and Photonics (2000).

[8] Kim, E. D., Choi, Y.-W., Kang, M.-S., and Choi, S. C., "Reverse-optimization alignment algorithm using zernike sensitivity," *Journal of the Optical Society of Korea* **9**(2), 68–73 (2005).